

# Batteries & Supercaps

Supporting Information

## **Fluorination of Ni-Rich Lithium-Ion Battery Cathode Materials by Fluorine Gas: Chemistry, Characterization, and Electrochemical Performance in Full-cells**

Ulf Breddemann<sup>+</sup>, Johannes Sicklinger<sup>+</sup>, Florian Schipper<sup>+</sup>, Victoria Davis, Anna Fischer, Korbinian Huber, Evan M. Erickson, Michael Daub, Anke Hoffmann, Christoph Erk, Boris Markovsky, Doron Aurbach,\* Hubert A. Gasteiger,\* and Ingo Krossing\*

# Contents

Experimental Section.....	3
Chemicals .....	3
Materials and Equipment.....	3
The fluorine fume hood .....	3
Ion Chromatography (IC).....	4
Ultrapure water .....	4
Fluoride selective electrode (FSE).....	4
FT-IR spectroscopy (IR).....	4
Powder X-Ray Diffraction (pXRD).....	4
Magic Angle Spinning – Nuclear Magnetic Resonance Spectroscopy (MAS-NMR) .....	4
Scanning electron microscopy (SEM).....	5
Conductivity and Press Density measurements.....	5
Thermo-gravimetric analyses (TGA) and Differential Thermal Analysis (DTA) .....	5
Electrochemical testing (Copy from Main Text, to have all data in one file).....	5
Experimental Procedure of Ni-NCM Fluorination .....	6
Direct Fluorination Setup for Ni-NCM materials.....	6
Analytics of the prepared fluorinated Ni-NCM CAM.....	7
Ion Chromatography (IC).....	7
Li and F content of the Fluorinated Ni-NCM materials.....	7
Powder X-Ray Diffraction (pXRD).....	12
pXRD data of (non-)Fluorinated NMC 811 and 851005 CAM.....	12
Infrared spectroscopy (IR) of (non-)NCM 811 and (non-)NCM 851005.....	14
<b>Thermogravimetric analyses (TGA) and Differential Thermal Analysis (DTA) .....</b>	<b>19</b>
Thermogravimetric Analysis coupled with Mass Spectrometry (TGA-MS).....	20
Subsequent calcination/heat treatment.....	20
Magic Angle Spinning – Nuclear Magnetic Resonance Spectroscopy (MAS-NMR) .....	21
<sup>7</sup> Li and <sup>19</sup> F MAS NMR Studies of (non-)Fluorinated NMC 811 and 851005 CAMs.....	21
Supplemental Information of <sup>7</sup> Li and <sup>19</sup> F MAS NMR Studies.....	22
Conductivity measurements of the Ni-rich materials.....	25
Press density measurements of the Ni-rich NCM CAMs.....	26
Thermodynamics of Fluorinated Uptake .....	27
References.....	28

## Experimental Section

### Chemicals

99.98 % fluorine gas was donated by Solvay Fluor GmbH, Germany, and the Ni-NCM (NCM 811 and NCM 851005) CAMs were contributed by BASF SE, Germany. **Attention!** Safety glasses, lab coat, and protective gloves must be worn at all times. **Caution!** Fluorine gas is an extremely hazardous material and should only be handled by trained personnel. All reactions should be carried out in a well-ventilated fume hood.

## Materials and Equipment

### The fluorine fume hood

The fluorine fume hood is a modified standard fume hood with its own discharge shaft and with an exhaust flow rate of 1200 m<sup>3</sup>/h. All of the walls in the fume hood as well as the full ventilation system are made of V4 A stainless steel. Fluorine gas is used from a 5 L fluorine gas bottle and stored inside the fume hood. For safety purposes, it is positioned in an additional V4 A stainless steel box coupled with a pressure regulator valve (Matheson Valves & Fittings Ltd.). One end of the pressure regulator valve is attached to the fluorine bottle using special O- Rings. The other end travels to the back of the fume hood and is connected to a *Monel vacuum line*, which can handle fluorine gas. All valves within the additional *V4 A stainless steel box* are equipped with length extended levers for easy access from outside of the box. There are three valves: the main bottle valve, the pressure-regulating valve, and a needle valve. (Figure S1).

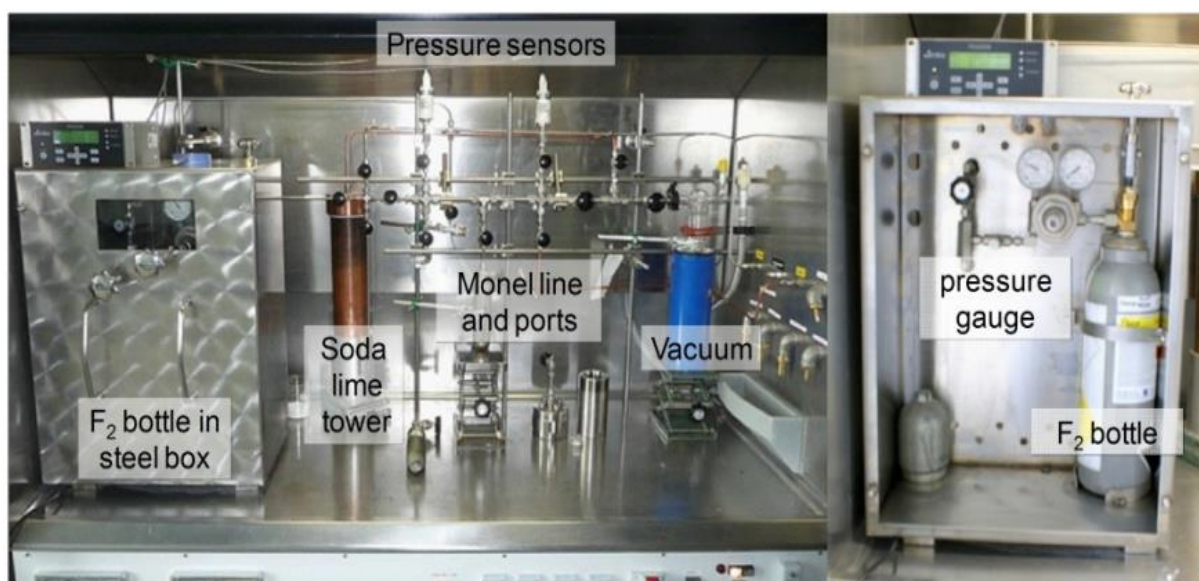


**Figure S1:** Left) Fluorine fume hood with the Monel vacuum line. Right) Inside of the fluorine bottle box.

## **Ion Chromatography (IC)**

IC measurements were carried out by *822 Compact IC plus* from *Metrohm* unit with a *Metrosep A Supp 5 – 250/4.0* high-performance separation anion column from *Metrohm* with a 1 mmol L<sup>-1</sup> NaHCO<sub>3</sub> and 3 mmol NaCO<sub>3</sub> in 10/90 % acetone/ultrapure water solution used as eluent. A *Metrosep C 4 - 100/4.0* high separation efficiency universal standard cation column from *Metrohm* were used with an eluent of 0.7 mmol 2,6-pyridinedicarboxylic acid and a 1.7 mmol nitric acid.

## **Ultrapure water**

Ultrapure water was product by PURELAB flex from the company Veolia Water Solutions & Technologies.

## **Fluoride selective electrode (FSE)**

The fluoride containing CAMs were thermally digested in an oxygen-steam stream at 1100 °C using a combustion unit (AQF-2100H, a1 envirotech). The resulting hydrogen fluoride was absorbed in an absorption solution (total ionic strength adjustment buffer, TISAB) and detected by means of a fluoride selective electrode (ISE 6.0502.150, Metrohm).

## **FT-IR spectroscopy (IR)**

IR measurements were measured on a Bruker alpha Fourier transform IR spectrometer arranged in an argon-filled glove box using a diamond ATR unit. The spectra were recorded in the range of 375 – 4000 cm<sup>-1</sup> and analyzed with the OPUS software package.

## **Powder X-Ray Diffraction (pXRD)**

pXRD data were collected with a Stoe Stadi P Powder diffractometer equipped with Mo-K<sub>α1</sub> radiation, a Ge(111) monochromator, and a silicon microstrip detector (Mythen 1k). The WinXPow package (STOE) was used for analysis and unit cell refinement. LeBail refinements were carried out with the program GSAS.<sup>[1],[2]</sup>

## **Magic Angle Spinning – Nuclear Magnetic Resonance Spectroscopy (MAS-NMR)**

<sup>7</sup>Li and <sup>19</sup>F magic angle spinning nuclear magnetic resonance experiments were performed on a Bruker DSX 500 solid-state NMR spectrometer running at a Larmor frequency of 194.40 MHz and 470.65 MHz for <sup>7</sup>Li and <sup>19</sup>F, respectively. The rotor synchronized Hahn Echo and rotor synchronized solid state Echo experiments were performed under magic angle spinning rates of 20 kHz to 30 kHz using a 2.5 mm MAS probe with an  $\omega_1/2\pi$  frequency of 125 kHz (i.e. a 90° pulse duration of 2 μs). and relaxation delays of 5 s (<sup>7</sup>Li) and 30 s (<sup>19</sup>F). All spectra were measured at room temperature, leading to sample temperatures of 300 K to 325 K, due to frictional heating of the magic angle spinning.

## Scanning electron microscopy (SEM)

SEM was performed on a Field Emission Gun-High Resolution Scattering Electron Microscope (FEG-HRSEM) SU8220 (Hitachi) with a Transmission Electrons (TE), Back Scattering Electrons (BSE), Secondary Electrons (SE), and and 2 EDX detectors (Bruker).

## Conductivity and Press Density measurements

Conductivity and Press Density measurements were carried out on a “*Loresta resistivity measurement unit*” from *Mitsubishi Chemical Analytech*.

## Thermo-gravimetric analyses (TGA) and Differential Thermal Analysis (DTA)

TGA and DTA was performed under nitrogen atmosphere on a STA 409 from the company *Netzsch*.

## Electrochemical testing (Copy from Main Text, to have all data in one file)

**Full-Cell (triplicate) Measurements:** Electrodes were fabricated as described elsewhere.\* Briefly, 80 % active cathode active material (pristine batch obtained from BASF SE, Germany) was mixed with 5 % Super C65 conductive carbon (Imerys, MTI corp. USA), 5 % TIMREX KS-6 graphite (Imerys, France) and 10 % Solef 5130 polyvinylidenedifluoride (PVDF) binder (Solev5130 from Solvay) in N-methylpyrrolidone (NMP), and cast onto an Al foil (Strem Chemicals Inc., USA) current collector at a loading of  $\sim 4.3 \text{ mg cm}^{-2}$ . Single layer pouch full-cells were fabricated with graphite anodes at a loading of  $\sim 2.8 \text{ mg cm}^{-2}$  with 20% excess capacity (negative to positive electrodes areal capacity ratio of N/P = 1.2), using Celgard PP 2500 separators and 350  $\mu\text{L}$  of BASF LP57 electrolyte (1 M  $\text{LiPF}_6$  ethylene carbonate: ethyl methyl carbonate, 3:7). Areal capacity of the full-cell:  $\sim 0.7 \text{ mAh cm}^{-2}$ , active electrode area:  $\sim 11.5 \text{ cm}^2$ , absolute pouch cell capacity:  $\sim 8 \text{ mAh}$ . The 1C rate for NCM 811 was set to correspond to  $180 \text{ mAh g}^{-1}$ . All cells were prepared in triplicate and the results were averaged. Formation procedure for cells: 1 cycle at C/15 followed by 4 cycles at C/10 at 30 °C. For the continuous cycling between 2.0 and 4.2 V, the cells were measured at 30 and 45 °C with a 0.5 C charge and 1 C discharge current and a 30 minutes CV-step at 4.2 V. Every 50 cycles, one cycle was measured during charge and discharge at 0.1 C. Electrochemical impedance spectra were measured using a Solartron battery test unit model 1470 coupled with the frequency response analyzer FRA-1250 from Solartron in the frequency range from 5 mHz to 0.1 MHz. Impedance spectra were collected during charge at 4.0 V after formation, 250 and 500 cycles of the continuous cycling test.

---

\* i.e., a) E. M. Erickson, H. Sclar, F. Schipper, J. Liu, R. Tian, C. Ghanty, L. Burstein, N. Leifer, J. Grinblat, M. Talianker et al., *Adv. Energy. Mater.* **2017**, *26*, 1700708; b) E. M. Erickson, F. Schipper, R. Tian, J.-Y. Shin, C. Er, F. F. Chesneau, J. K. Lampert, B. Markovsky, D. Aurbach, *RSC Adv* **2017**, *7*, 7116; c) F. Amalraj, M. Talianker, B. Markovsky, L. Burlaka, N. Leifer, G. Goobes, E. M. Erickson, O. Haik, J. Grinblat, E. Zinigrad et al., *J. Electrochem. Soc.* **2013**, *160*, A2220-A2233.

## Experimental Procedure of Ni-NCM Fluorination

### Direct Fluorination Setup for Ni-NCM materials

The setup consists of a 120 mL low pressure PFA (perfluoropolyether) batch reactor vessel equipped with a ¼" end cup fitting, a Stainless Steel Swagelok Tee-Type with a 0.5  $\mu\text{m}$  particle filter (connect to the end cup), and a Kel-F valve<sup>[3]</sup> (connected to the filter). These parts were assembled and connected to a *Monel* vacuum line of volume 66 mL (Figure S1) and checked for leaks (Figure S2). The reactor was evacuated and then filled with elemental fluorine gas at a total pressure of 1.1 bar for one hour to achieve equipment passivation. Once passivation was completed, the reactor was evacuated and the remaining reactive gases were neutralized over a soda lime tower. The setup was transferred into a solvent free dry box. In the dry box, the reactor vessel was opened and 7 g ( $\pm 0.04$  g) of Ni-NCM material (along with a Teflon-coated stir bar) was transferred into the batch reactor. The setup was removed from the dry box, connected to the *Monel* vacuum line to ensure the absence of any leaks and the inert gas in the PFA reactor vessel was pumped out. Next, the Monel Schlenk line was filled with  $\text{F}_2$  gas at pressures between 32 to 2200 mbar (or 0.1 to 5.5 mmol  $\text{F}_2$ ; cf. **Table S1** and **Table S2** for the pressure) and afterwards the valve to the evacuated PFA reactor vessel was opened and the gas expanded to a total pressure of 10 to 800 mbar. Immediately after exposure of the CAMs to the fluorine gas, the pressure began to drop, and stabilized within a few minutes indicating that the reaction was over. When the pressure stabilized (depending on the  $\text{F}_2$  amount added: at about 7-8 to 500 mbar), the vessel was backfilled with dry nitrogen gas until a total pressure of 1100 mbar was observed. After a reaction time of 1 hour, the remaining reactive gas was pumped out of the reactor vessel and neutralized in a soda lime tower. The closed setup was transferred into a solvent free dry box, opened, and the fluorinated material was transferred into a storage container until further use.

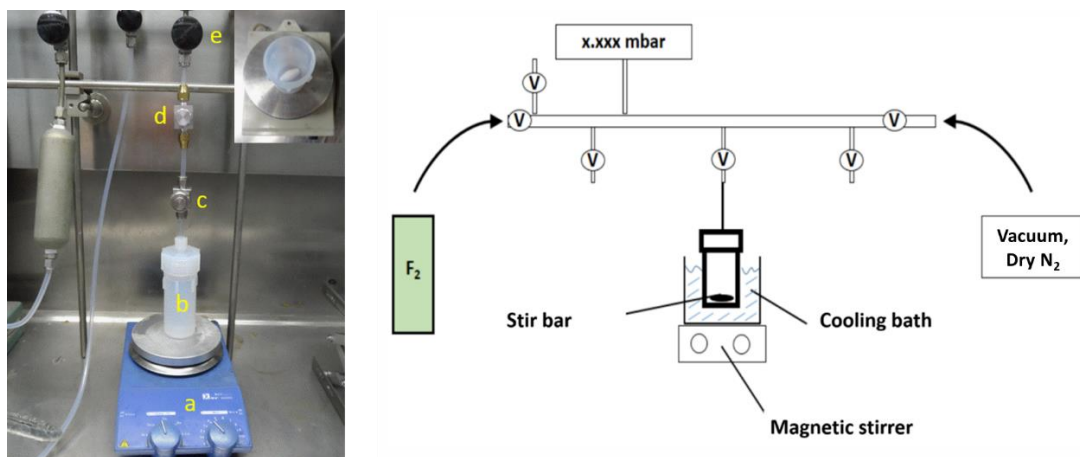


**Figure S2:** Left: The setup consists of a magnetic stirrer (a), a 120 mL low pressure PFA (perfluoroether) batch reactor vessel equipped with a ¼" end cup fitting (b), a Stainless Steel Swagelok Tee-Type with a 0.5  $\mu\text{m}$  particle filter (c), and a Kel-F valve (c). The vessel is connected to the Monel vacuum line (e). The top right inset picture shows the stir bar inside the vessel.

Right: Schematic drawing of the setup. The pre-passivated vacuum line has a volume of 66 mL and was filled with 32 to 2200 mbar F<sub>2</sub>-pressure.

## **Analytics of the prepared fluorinated Ni-NCM CAM**

### **Ion Chromatography (IC)**

IC measurements were carried out to determine the lithium and fluorine concentrations of the pristine and fluorinated Ni-NCM samples. A high purity multi-element ion chromatography cation and anion standard solution was used (Sigma-Aldrich) to assign the measured element and its concentration with precision. It is believed that after fluorination a LiF film forms at the surface of the cathode material as well as a possible formation of a metal fluorides such as NiF<sub>2</sub>, CoF<sub>2</sub>, and MnF<sub>2</sub>. The LiF film and the metal fluorides are soluble (in small amount) in water.<sup>[4],[5],[6],[7],[8],[9],[10],[11],[12],[13]</sup> The pristine and fluorinated samples were stored in a solvent free, argon filled dry box. In this dry box, an amount between 200 and 1000 mg fraction of the fluorinated samples was transferred into a PFA (perfluoroether) volumetric flask and transferred out of the box. The material was eluted with 250 mL ultrapure water, filtered (hydrophobic PTFE, 0.45 μm) before measurement.

### **Li and F content of the Fluorinated Ni-NCM materials**

To measure the water-soluble lithium (Li) and fluoride (F) concentration of the samples, ion chromatography (IC) studies were carried out for the (non-)fluorinated Ni-rich NCM CAMs. The presumably mainly formed LiF (v.i.) has a low, but reasonable solubility of 1.3 g L<sup>-1</sup> water. Thus, 0.2 to 1.0 g fractions of the fluorinated CAMs were eluted with 250 mL ultrapure water, filtered and the fluoride and lithium contents in the filtrate were investigated. The fluoride concentration of several samples was also verified by fluoride selective electrode (EA or FSE) analysis (labelled 'EA', Figure S3, Figure S4, Table S1, and Table S2).

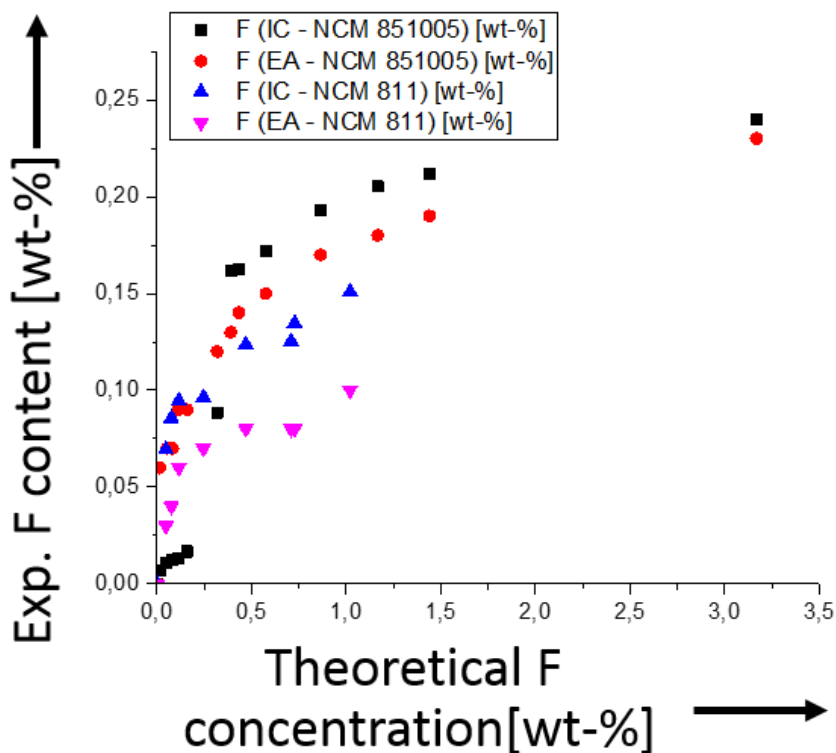


**Figure S3:** Plots of the water-soluble fluoride content of the treated CAMs in wt-% as a function of the applied amount of fluoride in wt-%. IC stands for ion chromatography and EA for a FSE determination.

First, one needs to note that the independent fluoride determinations by IC as well as FSE agree reasonably, so that we may suggest that through the aqueous extraction procedure, the full fluoride content is accessible. In general, one may state that especially lower fluorine amounts up to roughly 0.25 wt-% applied F are taken up by the CAMs more efficiently. Interestingly, the fluoride contents of NCM 811 and NCM 851005 develop differently as a function of the added  $F_2$  amount at F-contents larger than about 0.25 wt-% (theoretical uptake). On the NCM 811 CAM, from this applied  $F_2$  amount on, the system takes up further fluoride at a much slower rate. By contrast, the NCM 851005 system exhibits an almost asymptotic behavior approaching an apparently limiting fluoride content of about 0.24 wt-% (exp. fluoride content). This limiting F-content of the CAM is lower for NCM 811 by about 0.15 wt-%. Thus, apparently NCM 851005 contains a larger amount of the soluble base content ( $Li_2O$ ,  $LiOH$ ,  $LiOH \cdot H_2O$ ,  $Li_2CO_3$ ) that we expect to react preferentially with the  $F_2$  gas giving  $LiF$  as the main and relevant product.

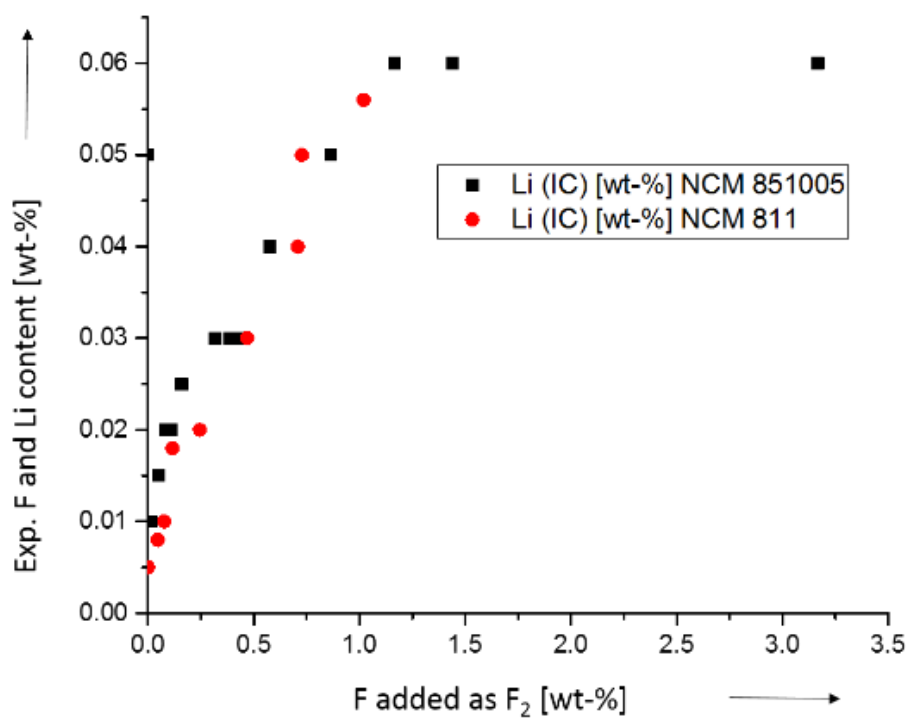


**Figure S4:** Plots of the water-soluble lithium content of the treated CAMs in wt-% as a function of the applied amount of fluoride in wt-%. IC stands for ion chromatography.

Lithium concentrations measured by IC showed comparable results. A strong increase of the observed lithium concentration as a function of the applied gaseous fluorine amount (theoretical F conc. in wt-%) was observed, until a limiting uptake of about 0.06 wt-% lithium was reached (exp. Li content).

**Table S1:** Ion chromatography (IC)<sup>a)</sup> and fluoride selective electrode (FSE)<sup>b)</sup> measurements for the (non-)fluorinated NCM 811 materials.

<b>Numeration of samples</b>	<b>p(F<sub>2</sub>) [mbar]</b>	<b>n F<sub>2</sub> [mmol]</b>	<b>Theoretical F concentration [wt-%]</b>	<b>IC<sup>a)</sup> Amount of F [wt-%]</b>	<b>FSE<sup>b)</sup> Amount of F [wt-%]</b>	<b>IC<sup>a)</sup> Amount of Li [wt-%]</b>
1	0	0.0	0	0	0	0.005
2	32	0.1	0.046	0.070	0.030	0.08
3	53	0.1	0.076	0.086	0.040	0.01
4	80	0.2	0.115	0.095	0.060	0.018
5	170	0.5	0.245	0.096	0.070	0.02
6	326	0.9	0.469	0.124	0.080	0.03
7	492	1.3	0.708	0.125	0.080	0.04
8	505	1.4	0.727	0.135	0.080	0.05
9	707	1.9	1.02	0.151	0.100	0.06

<sup>a)</sup> Since LiF has a solubility of 1.3 g L<sup>-1</sup> water, a between 200 and 1000 mg fraction of the fluorinated samples were eluted with 250 mL ultrapure water and the fluoride and lithium contents in the water were investigated by IC. <sup>b)</sup> As control experiments, selected fluorinated Ni-NCM 811 materials were tested for the fluoride content by fluoride selective electrode (FSE) after a complete work up for the analysis (here labelled FSE).

**Table S2:** Ion chromatograph (IC)<sup>a)</sup> and fluoride selective electrode (FSE)<sup>b)</sup> measurements for the (non-)fluorinated NCM 851005 materials.

<b>Numeration of samples</b>	<b>p(F<sub>2</sub>) [mbar]</b>	<b>n F<sub>2</sub> [mmol]</b>	<b>Theoretical F concentration [wt-%]</b>	<b>IC<sup>a)</sup> Amount of F [wt-%]</b>	<b>FSE<sup>b)</sup> Amount of F [wt-%]</b>	<b>IC<sup>a)</sup> Amount of Li [wt-%]</b>
1	0	0.0	0	0	0	0.05
2	10	0.0	0.014	0.007	0.06	0.01
3	36	0.1	0.052	0.011	0.07	0.015
4	56	0.2	0.081	0.013	0.07	0.02
5	76	0.2	0.109	0.013	0.09	0.02
6	110	0.3	0.158	0.017	0.09	0.025
7	220	0.6	0.317	0.088	0.12	0.03
8	270	0.7	0.389	0.162	0.13	0.03
9	300	0.8	0.432	0.162	0.14	0.03
10	400	1.1	0.576	0.172	0.15	0.04
11	600	1.6	0.864	0.193	0.17	0.05
12	810	2.2	1.166	0.205	0.18	0.06
13	1000	2.7	1.440	0.212	0.19	0.06
14	2200	5.9	3.168	0.240	0.23	0.06

<sup>a)</sup> Since LiF has a solubility of 1.3 g L<sup>-1</sup> water, a between 200 and 1000 mg fraction of the fluorinated samples were eluted with 250 mL ultrapure water and the fluoride and lithium contents in the water were investigated by IC. <sup>b)</sup> As control experiments, selected fluorinated Ni-NCM 851005 materials were tested for the fluoride content by fluoride selective electrode (FSE) after a complete work up for the analysis (here labelled FSE).

## Powder X-Ray Diffraction (pXRD)

### pXRD data of (non-)Fluorinated NMC 811 and 851005 CAM

In a dry box, the material was transferred into a capillary (length: 80 mm, outside-diameter: 0.3 mm, and a wall thickness: 0.01 mm), then air-tight sealed and transferred out of the dry box for further sealing (with a lighter) of the capillary until an average length of 2 cm.

pXRD measurements were carried out for the pristine and the few fluorinated NCM 811 and 851005 samples (Figure S5 and Table S3). pXRD data for the low and high fluorinated NCM 811 and 851005 materials showed almost identical powder diffractograms and LeBail fittings (only 851005 CAMs) suggested lattice parameters very close to that of the rhombohedral cell (space group  $R\bar{3}m$ ) of pristine NCM 811 and 851005 material (see below).

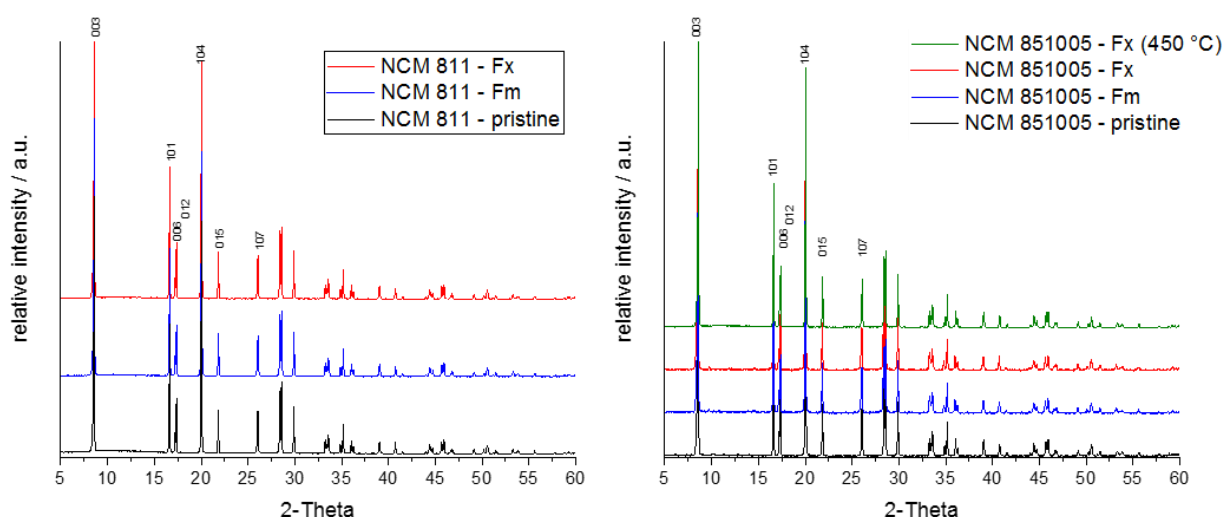


**Figure S5:** pXRD data of (non-)fluorinated Ni-NCM CAM, measured with  $\alpha$  Mo- $K_{\alpha 1}$  radiation with full powder traces with Miller indices [hkl] assigned to reflexes up to  $30^\circ$   $2\theta$ . Left) NCM 811 CAM and right) NCM 851005 CAM.

**Table S3:** pXRD data analysis (Mo- $K_{\alpha 1}$  radiation) and LeBail fitting of the (non-)fluorinated Ni-rich CAMs.

Method	Cell parameters	NCM 811			NCM 851005			
		pristine	0.105 wt-% label: F <sub>m</sub>	0.126 wt-% label: F <sub>x</sub>	pristine	0.06 wt-% label: F <sub>m</sub>	0.23 wt-% label: F <sub>x</sub>	0.23 wt-% heated to 450 °C label: F (450 °C)
STOE	$a$ [Å]	2.8716(3)	2.87124(23)	2.8719(3)	2.8715(3)	2.8707(4)	2.8710(3)	2.87181(24)
STOE	$c$ [Å]	14.2076(13)	14.2007(11)	14.2035(12)	14.1911(14)	14.2258(18)	14.2318(15)	14.1832(10)
STOE	$c/a$	4.9476	4.9458	4.9457	4.9421	4.9556	4.9571	4.9388
STOE	$V$ [Å <sup>3</sup> ]	101.458(13)	101.387(11)	101.454(12)	101.335(12)	101.527(17)	101.594(15)	101.301(11)
LeBail	$a$ [Å]		no Data		2.87186(3)	2.87177(3)	2.87180(4)	2.871728(17)
LeBail	$c$ [Å]		no Data		14.1959(2)	14.2296(3)	14.2331(3)	14.18333(14)
LeBail	$c/a$		no Data		4.9431	4.9550	4.9562	4.9390
LeBail	$V$ [Å <sup>3</sup> ]		no Data		101.396(2)	101.626(2)	101.657(3)	101.297(1)

pXRD was carried out for the pristine and few selected fluorinated Ni-NCM materials. pXRD data for the low and high fluorinated NCM 811 materials showed almost identical powder diffractograms and LeBail fitting suggested lattice parameters very close to that of the rhombohedral cell (space group  $R\bar{3}m$ ) of pristine NCM 851005 material (Figure S6 and Figure S7).

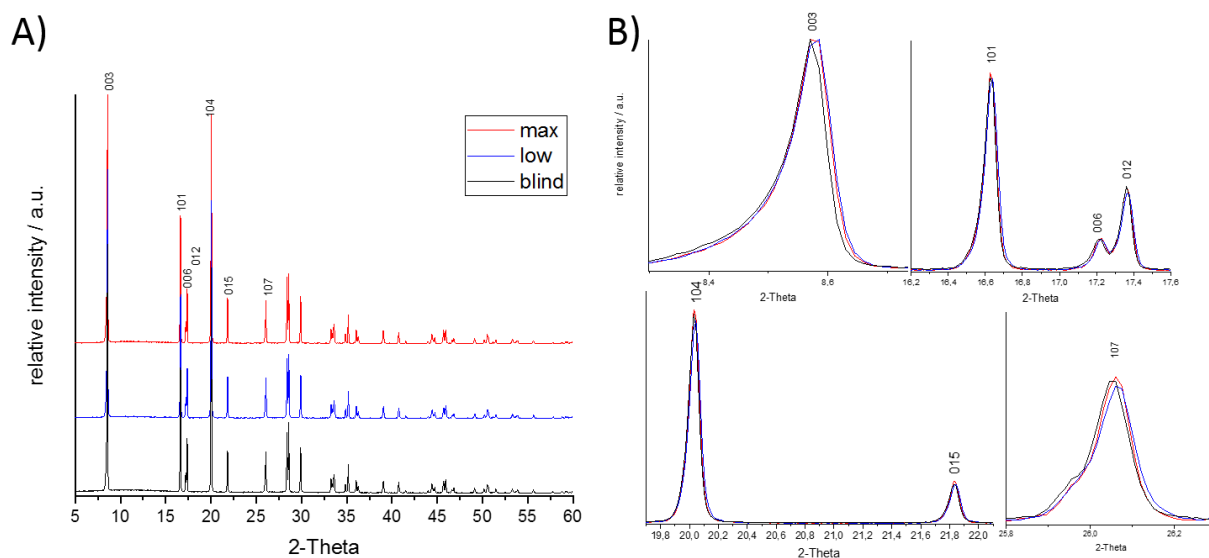


**Figure S6:** pXRD traces of (non-)fluorinated NCM 811 CAM, measured with Mo- $K_{\alpha 1}$  radiation. A) Full powder traces with Miller indices [hkl] assigned to reflexes up to  $30^\circ 2\theta$ ; B) detail between  $8.2$  to  $8.8$ ,  $16.0$  to  $17.6$ ,  $19.7$  to  $22.2$ , and  $25.8$  to  $26.3^\circ 2\theta$ .

pXRD data of (non-)fluorinated NCM 851005 CAM showed for all materials the same a-axis value. The c-axis showed for the fluorinated samples the same value, where the value of the pristine and high fluorinated and over calcination material showed almost identical lattice parameters (Figure S7).

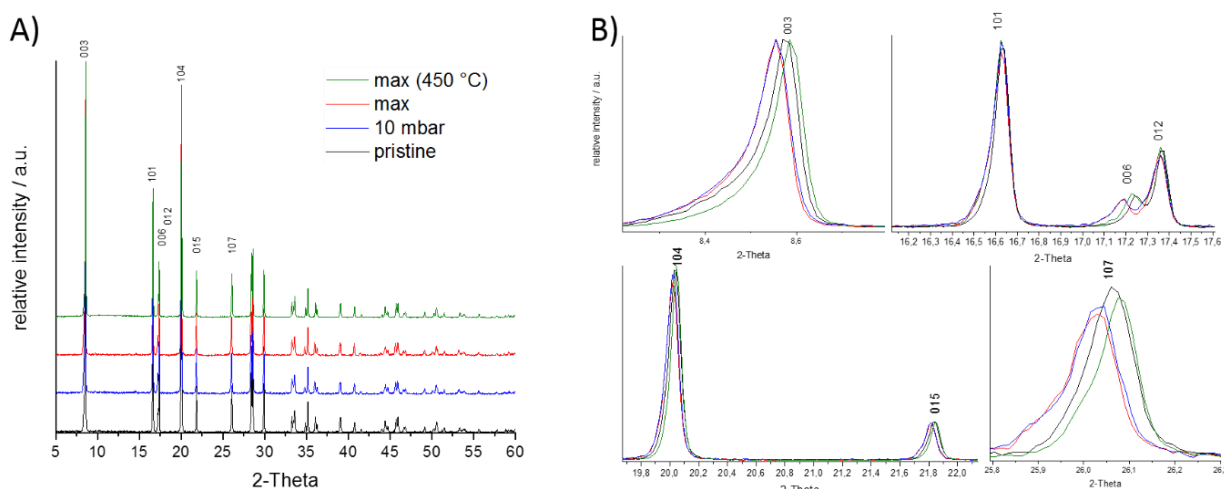


**Figure S7:** pXRD traces of (non-)fluorinated NCM 851005 CAM, measured with Mo- $K_{\alpha 1}$  radiation. A) Full powder traces with Miller indices [HKL] assigned to reflexes up to  $30^\circ 2\theta$ ; B) detail between  $8.2$  to  $8.8$ ,  $16.0$  to  $17.6$ ,  $19.7$  to  $22.2$ , and  $25.8$  to  $26.3^\circ 2\theta$ .

## Infrared spectroscopy (IR) of (non-)NCM 811 and (non-)NCM 851005

ATR-IR spectra of the bulk (non-)fluorinated NCM 811 and (non-)NMC 851005 CAMs indicated no formation of metal fluorine compounds.<sup>[14]</sup> All obtained IR spectra appeared to be identical showing the typical characteristic bands for NCM 811 and NCM 851005 CAMs.

**Table S4:** Experimental IR frequencies (range 350 cm<sup>-1</sup> to 4000 cm<sup>-1</sup>) of (non-)fluorinated NCM 811 materials. The samples are ordered by increasing theoretical F-content. The samples 270 mbar and 400 mbar were not measured.

Pristine	0.05 wt-% F (lable: 23-32)	0.06 wt-% F (lable: 38-53)	0.07 wt-% F (lable: 505)	0.11 wt-% F (lable: 57)	0.11 wt-% F (lable: 122)	0.11 wt-% F (lable: 363)
			961 (13)			
			938 (17)			
	903 (10)		903 (22)		901 (12)	
860 (21)	863 (28)	868 (28)	865 (35)	861 (18)	868 (26)	
	856 (28)	860 (28)	854 (37)		859 (26)	859 (16)
						848 (18)
	836 (32)	839 (32)	837 (37)	839 (18)		
828 (27)				828 (20)	825 (34)	823 (21)
	817 (36)		810 (41)	816 (24)	809 (38)	
			800 (41)			802 (26)
	798 (40)	796 (38)			792 (40)	792 (26)
	782 (42)	787 (38)	782 (41)			784 (29)
774 (42)		778 (40)			775 (42)	
	773 (42)	772 (40)		771 (33)		
763 (40)		761 (40)		763 (33)	762 (40)	762 (29)
		755 (40)				
569 (100)	571 (100)	569 (100)	572 (100)	569 (100)	569 (100)	570 (100)
541 (90)	544 (84)	545 (87)	540 (89)	543 (82)	543 (86)	544 (87)
534 (89)		535 (87)		537 (82)	536 (88)	
			528 (83)	529 (84)		
		501 (64)		510 (76)		
				497 (64)		
				487 (60)		482 (47)
476 (44)	477 (46)	471 (43)	476 (48)		473 (48)	
	466 (42)		462 (43)	465 (47)		
		457 (32)		456 (40)		457 (32)
444 (29)	449 (30)	443 (28)		448 (40)		441 (24)
434 (25)	438 (28)	436 (26)		437 (38)	435 (34)	430 (24)
424 (19)	424 (24)		427 (28)	430 (33)	425 (26)	419 (16)
	414 (18)	409 (19)	410 (22)	411 (22)		410 (18)
						404 (16)

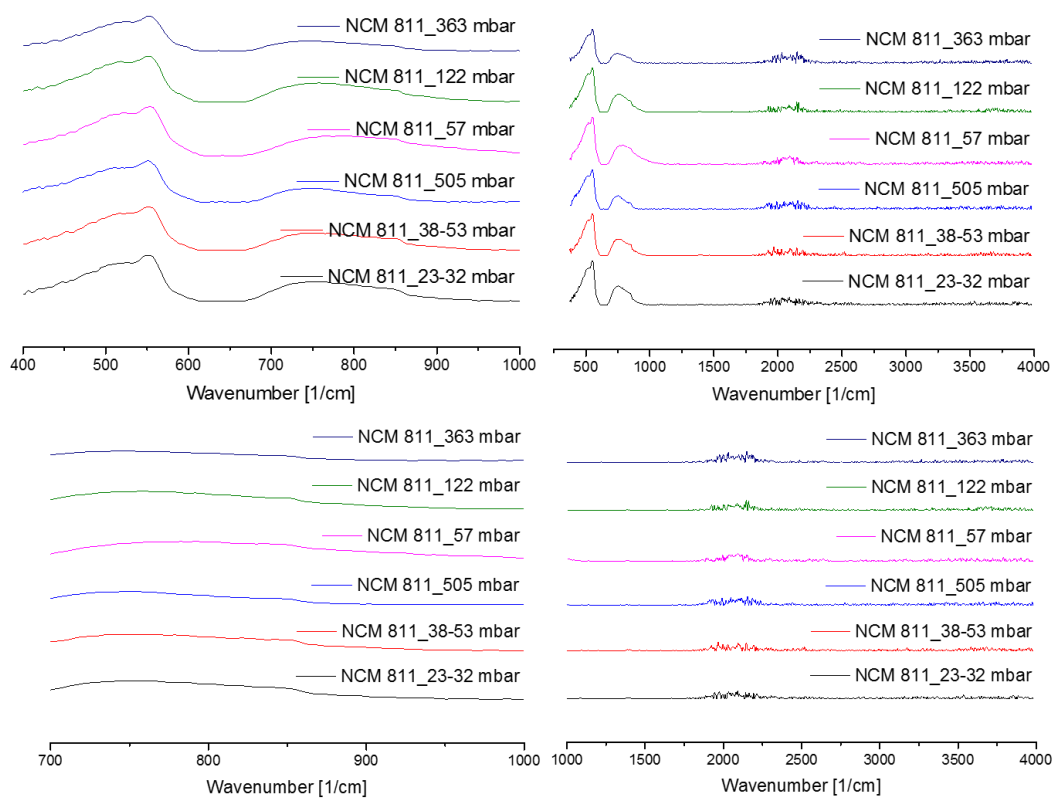


**Figure S8:** ATR-IR Spectra of the pristine and fluorinated NCM 811 materials (with a baseline correction), where 32-32 (0.05 wt-%), 38-53 (0.06 wt-% F), 505 (0.07 wt-% F), 57 (0.11 wt-% F), 122 (0.11 wt-% F), and 363 (0.11 wt-% F).

**Table S5:** Experimental IR frequencies (range 350 cm<sup>-1</sup> to 4000 cm<sup>-1</sup>) of (non-)fluorinated NCM 851005 materials. The samples are ordered by increasing theoretical F-content. The sample 270 mbar and 400 mbar were not measured.

pristine	0.06 wt-% F	0.11 wt-% F	0.013 wt-% F	0.013 wt-% F	0.017 wt-% F	0.088 wt-% F	300 wt-% F	0.162 wt-% F	0.205 wt-% F	0.212 wt-% F	0.240 wt-% F
3705 (23)	3705 (23)	3704 (23)	3706 (23)	3706 (23)	3705 (23)	3705 (23)	3706 (23)	3705 (23)	3705 (23)	3705 (22)	3705 (23)
3677 (16)	3677 (17)	3676 (15)	3676 (16)	3676 (16)	3676 (16)	3677 (16)	3674 (15)	3676 (16)	3677 (16)	3676 (16)	3677 (17)
///	3664 (10)	3666 (8)	///	///	///	///	///	///	///	///	///
///	1614 (10)	1620 (8)	///	///	///	///	///	///	///	///	///
1368 (22)	1368 (23)	1368 (22)	1368 (22)	1368 (22)	1367 (22)	1368 (22)	1367 (22)	1368 (21)	1368 (22)	1368 (22)	1367 (23)
1286 (28)	1282 (30)	1286 (28)	1287 (28)	1285 (28)	1285 (28)	1286 (29)	1286 (29)	1387 (22)	1285 (28)	1285 (28)	1285 (29)
///	///	///	///	///	///	///	///	1286 (28)	///	///	///
1175 (41)	///	///	///	///	///	///	///	///	///	///	///
1158 (43)	///	///	///	///	///	///	///	///	///	///	///
1124 (24)	1227 (25)	1227 (24)	1227 (24)	1226 (24)	1226 (24)	1226 (24)	1226 (24)	1226 (24)	1226 (24)	1225 (24)	1227 (24)
///	1173 (42)	1175 (42)	1174 (42)	1174 (42)	1173 (41)	1174 (42)	1175 (42)	1173 (42)	1174 (42)	1173 (42)	1175 (42)
///	1159 (44)	1158 (43)	1158 (43)	1160 (43)	1158 (43)	1157 (43)	1156 (43)	1158 (42)	1158 (43)	1158 (43)	1159 (43)
1086 (46)	1086 (47)	1086 (46)	1088 (46)	1087 (46)	1086 (46)	1085 (46)	1085 (46)	1087 (46)	1086 (46)	1086 (46)	1086 (46)
///	1075 (sh)	1074 (sh)	1074 (sh)	1075 (sh)	1074 (sh)	///	1075 (sh)	///	1076 (sh)	1076 (sh)	1076 (sh)
1064 (sh)	1062 (sh)	1062 (sh)	1060 (sh)	1066 (sh)	///	1065 (sh)	///	///	///	///	///
///	///	///	///	1055 (sh)	1055 (sh)	///	///	1053 (sh)	///	///	///
///	///	1030 (sh)	///	///	///	///	1038 (sh)	///	///	1041 (sh)	1047 (sh)
918 (8)	920 (9)	918 (8)	920 (8)	921 (8)	919 (8)	920 (8)	918 (8)	919 (8)	919 (8)	917 (8)	920 (8)
883 (27)	883 (28)	884 (27)	884 (27)	884 (27)	885 (27)	884 (27)	882 (27)	883 (27)	884 (27)	884 (27)	883 (27)
858 (sh)	861 (sh)	859 (sh)	859 (sh)	859 (sh)	858 (sh)	859 (48)	860 (48)	857 (sh)	858 (sh)	860 (sh)	858 (sh)
847 (60)	846 (60)	846 (60)	849 (59)	847 (59)	846 (60)	847 (60)	848 (60)	858 (59)	846 (59)	846 (60)	848 (60)
816 (35)	817 (37)	817 (35)	815 (35)	818 (36)	817 (35)	818 (36)	819 (36)	816 (35)	816 (35)	818 (35)	816 (36)
803 (34)	808 (35)	808 (34)	807 (33)	807 (33)	807 (34)	806 (34)	807 (34)	808 (34)	807 (34)	807 (36)	807 (34)
///	///	///	///	///	///	799 (29)	///	///	///	///	///
759 (60)	760 (61)	759 (59)	759 (59)	759 (60)	760 (60)	759 (60)	759 (60)	759 (60)	759 (60)	759 (60)	758 (60)
742 (48)	742 (49)	742 (47)	741 (47)	741 (47)	742 (47)	742 (48)	740 (47)	740 (48)	741 (48)	741 (48)	742 (48)

719 (38)	720 (40)	720 (38)	719 (40)	720 (38)	718 (39)	719 (39)	718 (38)	719 (38)	721 (38)	719 (38)	718 (39)
///	///	705 (sh)	706 (sh)	708 (sh)	711 (sh)	708 (33)	709 (sh)	707 (32)	708 (33)	707 (sh)	708 (sh)
680 (20)	680 (21)	680 (20)	680 (20)	680 (20)	681 (20)	681 (20)	///	680 (20)	679 (20)	680 (20)	680 (20)
///	///	///	///	///	///	///	669 (17)	///	///	///	///
568 (100)	567 (100)	569 (100)	569 (100)	568 (100)	568 (100)	568 (100)	567 (100)	567 (100)	567 (100)	566 (100)	567 (100)
///	///	///	///	///	///	///	557 (sh)	///	558 (sh)	///	552 (90)
532 (83)	532 (83)	532 (83)	531 (83)	531 (83)	531 (83)	531 (83)	531 (83)	533 (83)	532 (83)	531 (84)	531 (83)
522 (75)	519 (76)	519 (75)	517 (75)	517 (75)	518 (75)	517 (75)	517 (75)	520 (76)	518 (75)	518 (75)	517 (75)
///	///	///	///			499 (sh)	508 (sh)		503 (sh)	509 (70)	509 (sh)
487 (57)	487 (58)	486 (57)	486 (56)	485 (57)	485 (57)	486 (6)	487 (57)	485 (57)	486 (57)	485 (57)	485 (57)
461 (42)	464 (43)	464 (41)	463 (42)	464 (41)	463 (41)	462 (41)	462 (41)	463 (41)	465 (42)	463 (42)	463 (42)
///	///	///	461 (sh)	///	///	///	///	///	///	///	///
///	454 (sh)	///	///	///	452 (sh)	453 (sh)	451 (sh)	///	450 (sh)	453 (sh)	451 (sh)
///	444 (sh)	439 (sh)	438 (sh)	439 (sh)	438 (sh)	437 (sh)	437 (sh)				
426 (26)	425 (28)	424 (27)	426 (26)	426 (26)	424 (27)	424 (26)	426 (26)	425 (26)	424 (26)	425 (26)	425 (27)
411 (15)	415 (22)	415 (21)	415 (21)	414 (22)	414 (21)	413 (21)	414 (21)	413 (21)	416 (21)	414 (21)	414 (21)
///	398 (10)	399 (9)	///	399 (9)	///	///	///	///	///	///	///

---

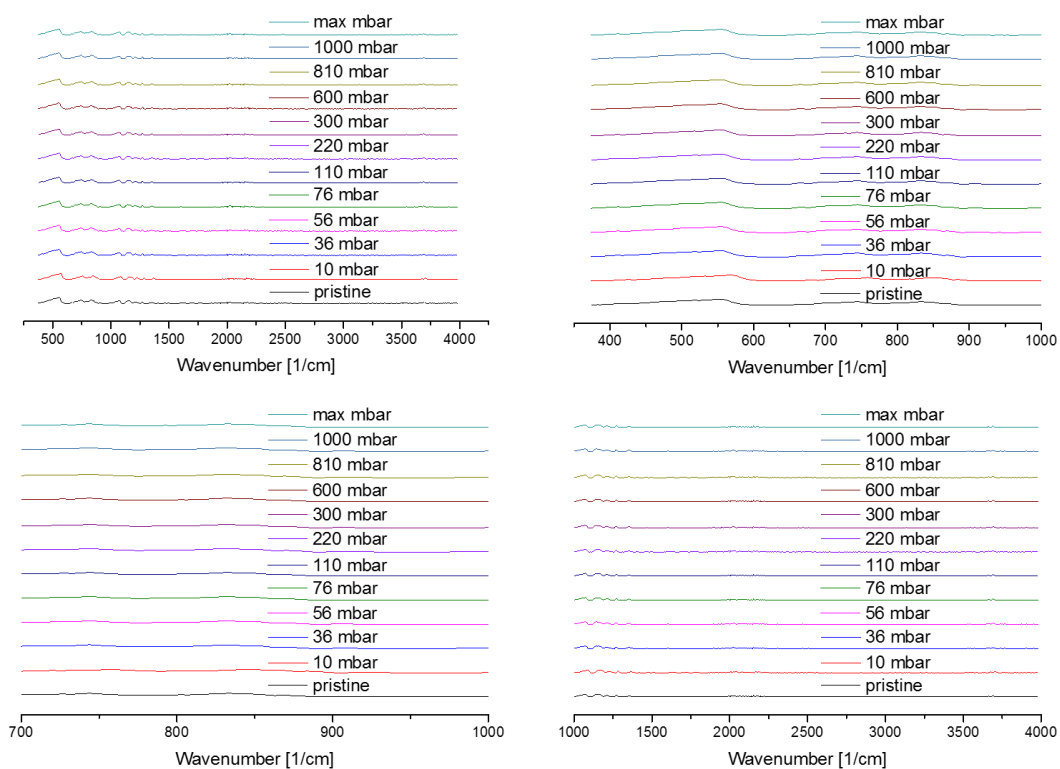


**Figure S9:** ATR-IR Spectra of the pristine and fluorinated NCM 851005 materials (with a baseline correction), where 10 mbar (0.06 wt-% F), 36 mbar (0.11 wt-% F), 56 mbar (0.013 wt-% F), 76 mbar (0.013 wt-% F), 110 mbar (0.017 wt-% F), 220 mbar (0.088 wt-% F), 300 mbar (300 wt-% F), 600 mbar (0.162 wt-% F), 810 mbar (0.205 wt-% F), 1000 mbar (0.212 wt-% F), and max mbar (0.240 wt-% F).

## Thermogravimetric analyses (TGA) and Differential Thermal Analysis (DTA)

**Does Fluorination alter the Thermal stability of Ni-rich NCM CAMs...?** The thermal stability of the (non-) fluorinated Ni-rich NCM CAMs is crucial for a long battery lifetime. To study the thermal stability, thermogravimetric analysis (TGA) and differential thermal analysis (DTA) measurements were carried out. The materials were placed in a thermogravimetric analyser and heated to 650 °C at 10 °C/min under nitrogen gas. The pristine material was also characterized under the same conditions. TGA measurements showed for the (non-)fluorinated NCM 811 CAM a mass loss between 0.16 to 0.81 % (Figure S10), where the DTA measurements shown no change in thermal stability (Figure S10). TGA measurements showed for the (non-)fluorinated NCM 851005 CAM a mass loss between 0.1 to 1.0 % (Figure S11), where the DTA measurements shown no change in thermal stability (Figure S11).

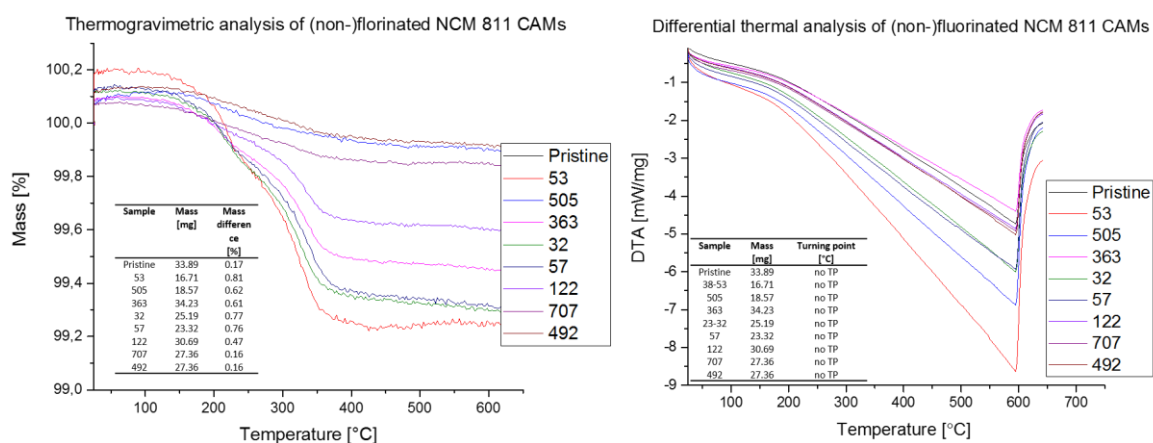


**Figure S10:** TGA and DTA results of (non-) fluorinated Ni-rich NCM 811 CAMs.

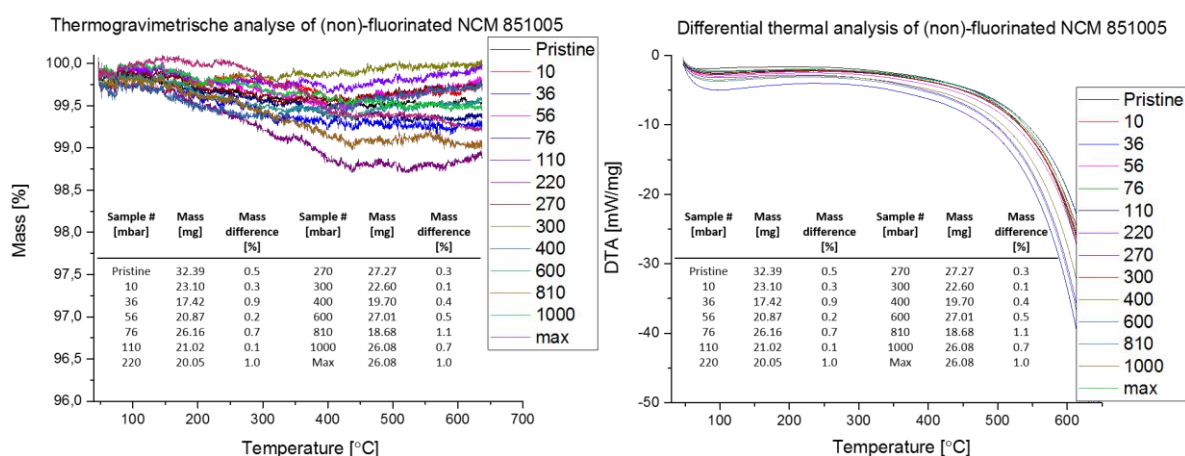


**Figure S11:** TGA and DTA results of (non-) fluorinated NCM 851005 CAMs, where 10 mbar (0.06 wt-% F), 36 mbar (0.11 wt-% F), 56 mbar (0.013 wt-% F), 76 mbar (0.013 wt-% F), 110 mbar (0.017 wt-% F), 220 mbar (0.088 wt-% F), 300 mbar (0.30 wt-% F), 600 mbar (0.162 wt-% F), 810 mbar (0.205 wt-% F), 1000 mbar (0.212 wt-% F), and max mbar (0.240 wt-% F).

### **Thermogravimetric Analysis coupled with Mass Spectrometry (TGA-MS)**

To analyze thermally labile surface species on the materials, the samples were analyzed by TGA-MS using a Mettler Toledo TGA/DSC 1 (*Mettler Toledo*, Switzerland) coupled to a ThermoStar MS (*Pfeiffer Vacuum*, Germany). Inside the glovebox, 30 mg to 35 mg of the sample were filled into a 150  $\mu\text{l}$  aluminum oxide crucible and transported to the device inside an airtight glass bottle. The sample was at pace inserted into the device (exposure time to ambient air less than 1 min) and heated stepwise at a rate of  $10 \text{ K min}^{-1}$  to  $1125 \text{ }^\circ\text{C}$  under argon. This temperature was retained for another 30 min. At  $120 \text{ }^\circ\text{C}$  and  $450 \text{ }^\circ\text{C}$  the temperature was hold constant for 30 min to ensure a clear separation of the desorbing phases. The temperature profile, which contains further isothermal steps at 25 and  $1125^\circ\text{C}$ , is illustrated in the TGA-MS results. A constant Ar flow of  $60 \text{ ml min}^{-1}$  forces the desorption products to the MS. The weight loss and the associated mass signals are recorded.

### **Subsequent calcination/heat treatment**

The effect of a calcination under Ar at  $400 \text{ }^\circ\text{C}$  and  $450 \text{ }^\circ\text{C}$  was investigated. These conditions are from now on referred to as “Ar  $400 \text{ }^\circ\text{C}$ ” and “Ar  $450 \text{ }^\circ\text{C}$ ”. The total gas flow was  $1 \text{ L min}^{-1}$ . In each case, the target temperature was held for 1 h.

## Magic Angle Spinning – Nuclear Magnetic Resonance Spectroscopy (MAS-NMR)

### $^7\text{Li}$ and $^{19}\text{F}$ MAS NMR Studies of (non-)Fluorinated NMC 811 and 851005 CAMs

$^7\text{Li}$  and  $^{19}\text{F}$  MAS NMR Studies were carried out for (non-)fluorinated NMC 811 and 851005 CAMs for the pristine, low (average F-concentration: 0.108 wt-%<sub>(NMC811)"/0.0335 wt-%<sub>(NMC 851005)</sub>), and high (average F-concentration: 0.126 wt-%<sub>(NMC 811)"/0.24 wt-%<sub>(NMC 851005)</sub>) fluorinated NMC CAMs (Figure S12).</sub></sub>

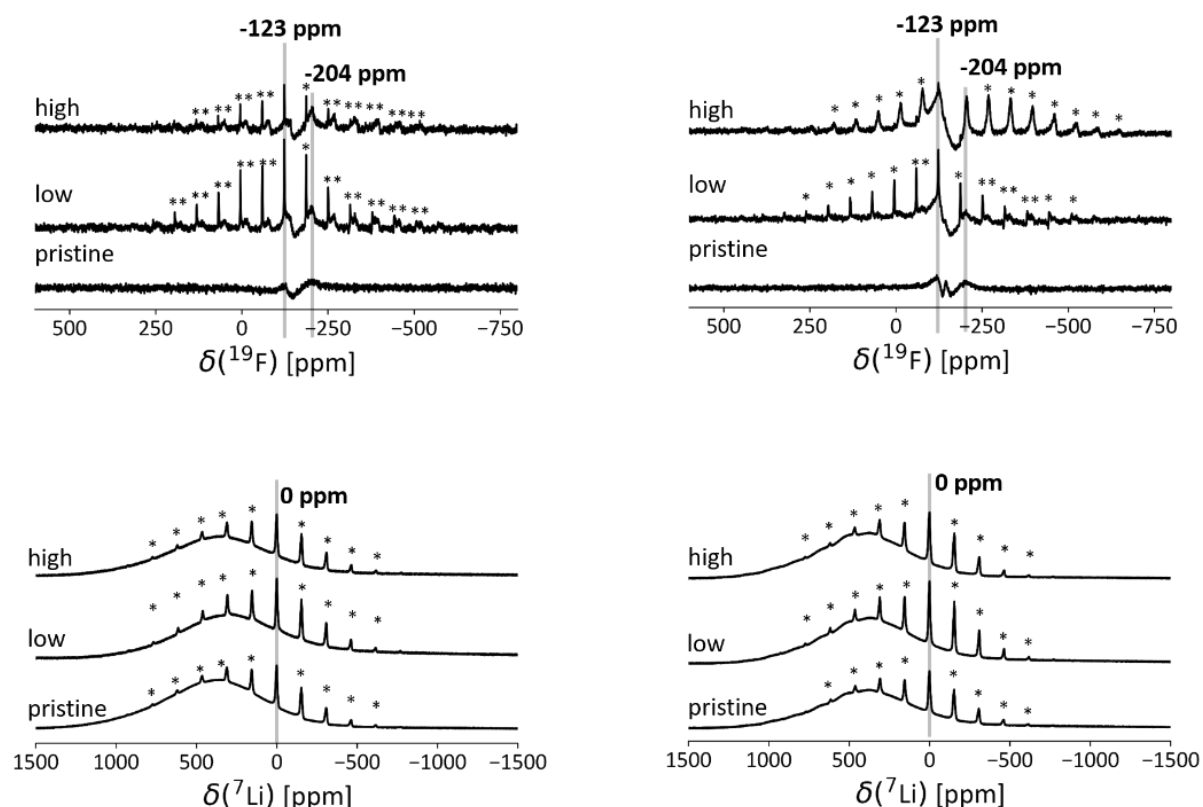


**Figure S12:**  $^{19}\text{F}$  and  $^7\text{Li}$  MAS NMR (30 kHz spinning,  $^{19}\text{F}$  background subtracted); left) (non-)fluorinated NMC 811 and right) (non-)fluorinated NMC 851005 of pristine, low and high fluorinated NMC CAMs. Spinning sidebands are marked by\*.

The  $^{19}\text{F}$  rotor-synchronized Hahn-Echo MAS NMR spectra of all fluorinated NMC samples show a signal at an isotropic shift of  $-204.0$  ppm that fits very well to the signal of neat solid LiF at  $-204.5$  ppm (Figure S15). There is a second very small signal at  $-123$  ppm originating from traces of PTFE ( $-123$  ppm) in the samples (probably from the stir bar). The distortion of the spectra around  $-100$  to  $-200$  ppm results from incomplete subtraction of the background signal originating from the PTFE parts of the MAS probe (Figure S14).

In the rotor synchronized solid-echo  $^7\text{Li}$  spectra recorded at 30 KHz MAS a sharp signal with well resolved spinning sidebands is observed for all fluorinated samples. Its isotropic shift is identical to that of neat LiF at  $-0.3$  ppm (Figure S12 and Figure S16). Additionally, in all the  $^7\text{Li}$  spectra a very broad signal that does not split into spinning sidebands with a width of about  $-500$  to  $+1000$  ppm

could be found. It was assigned to the lithium atoms in the bulk material of the Ni-rich material with the highest spatial proximity to the unpaired electrons.

Furthermore, it is shifted by more than 300 ppm as compared to neat LiF due to the unpaired electron spin density transferred from the neighbor layered Ni-rich NCM oxide to the nucleus (Fermi contact shift). Its linewidth originates from nucleus-electron dipolar interactions as well as a distribution of Fermi contact shifts.<sup>[15]</sup>

The observed chemical shifts in both the  $^{19}\text{F}$  and  $^7\text{Li}$  spectra perfectly match the ones observed for neat LiF and thus were assigned to arise from LiF.

However, the spinning sidebands envelope of both, the  $^7\text{Li}$  and  $^{19}\text{F}$  signal, is strikingly broadened in comparison to that of neat LiF (about 150 kHz for  $^7\text{Li}$  and 200 kHz for  $^{19}\text{F}$ ). As the dipole-dipole coupling of  $^7\text{Li}$  and  $^{19}\text{F}$  should be comparable to that in neat LiF and should in general not exceed 100 kHz, the line broadening can only be explained by dipole-dipole interaction of the observed nuclei with the electron spin of the Ni-rich NCM oxide materials. This interaction requests a close spatial proximity. However, since the lines have isotropic shifts identical to neat solid LiF (i. e. no Fermi contact shift is observed) the LiF causing this line is not present within the bulk but rather coating the Ni-rich NCM material.<sup>[32]</sup>

### Further Information on the $^7\text{Li}$ and $^{19}\text{F}$ MAS NMR Studies

**Identification of LiF by MAS-NMR Spectroscopy:** The  $^{19}\text{F}$  Hahn-Echo MAS-NMR spectra (Figure **S13**) of low and high fluorinated CAMs were measured at a spinning frequency of 30 kHz. There is a large background signal originating from the PTFE, which is far outside the NMR coil and hence experiences smaller pulse angles than the sample. It is thus not well refocused by the Echo experiment- However, its signal is not entirely suppressed and its phasing is not compatible with that of the sample. Thus, the background signal was recorded separately and subtracted (as shown for high fluorinated NCM 811 in Figure S14). Unfortunately, the actual shape slightly changes as the sample is removed, leading to a visible distortion of the spectra around  $-100$  ppm to  $-200$  ppm (Figure S13). The spectra of all samples show a signal with an isotropic shift of  $-204.0$  ppm, which very well fits to the signal of neat LiF at  $-204$  ppm that was recorded for comparison. The FWHM (full width at half maximum) of the spinning sidebands envelope is about 200 kHz, when measured at 470.65 MHz. This is a significantly increased value when compared to the spinning sidebands envelope of neat LiF, as easily is seen in the comparison of both spectra in Figure **S15**. The origin of this increased width will be discussed jointly with the lithium spectra. The spectra also show traces of PTFE ( $-123$  ppm) contained in the sample (likely from the stir bar used), which could be identified by its chemical shift and its very sharp signal.

The  $^7\text{Li}$  solid-state Echo MAS-NMR spectra of the high fluorinated samples are shown in Figure **S16** and compared to a spectrum of neat LiF, showing an isotropic shift of  $-1.4$  ppm. Both samples exhibit a sharp signal at an identical isotropic shift. The spinning sidebands envelope of this signal was also strikingly broadened in comparison to neat LiF to about 150 kHz.

A pristine sample of the Ni-rich NCM CAM (Figure S12) also showed a similar sharp signal in the same region that could be assigned to  $\text{Li}_2\text{CO}_3$ . The existence of a  $\text{Li}_2\text{CO}_3$  layer is commonly known for NCM cathode materials.<sup>[16]</sup> Already by qualitative comparison of the intensities, the amount of the coating lithium species was easily found to be significantly increased in all measured fluoridated samples. As the observed chemical shifts in both the  $^{19}\text{F}$  and  $^7\text{Li}$  spectra perfectly match the ones observed for neat LiF and both lines exhibit the same broadening of the sideband pattern they were assigned to arise from LiF.

Additionally, a very broad signal that does not split into spinning sidebands with a width of about 200 kHz to 300 kHz could be found in every  $^7\text{Li}$  MAS NMR spectrum. Due to the broadness, the lack of splitting into spinning sidebands and its huge integral value, it was assigned to the lithium atoms in the bulk material of the Ni-rich NCM CAMs with the highest spatial proximity to the unpaired electron spins. Furthermore, it is shifted by more than 300 ppm as compared to neat LiF due to the unpaired electron spin density transferred from the neighbored layered Ni-rich NCM oxide to the nucleus (Fermi contact shift). Its linewidth originates from nucleus-electron dipolar interactions as well as a distribution of Fermi contact shifts.<sup>[17]</sup>

The huge increase in the width of the spinning sideband patterns observed in  $^7\text{Li}$  and  $^{19}\text{F}$  spectra of all samples cannot be explained by dipole-dipole coupling of  $^7\text{Li}$  and  $^{19}\text{F}$ , as this should be comparable to the one in neat LiF and should in general not exceed 100 kHz. It can only be explained by interaction of the observed nuclei with the electron spin of the layered Ni-rich NCM oxide. This interaction requests a close spatial proximity. However, the lines have isotropic shifts identical to neat solid LiF, i.e. no Fermi contact shift is observed as would be expected for material within the bulk. Hence, the LiF causing this line is not present within the bulk but rather coating the Ni-rich NCM material as likewise reported by Ménétrier et. al. and Murakami et. al.<sup>[17],[18]</sup>

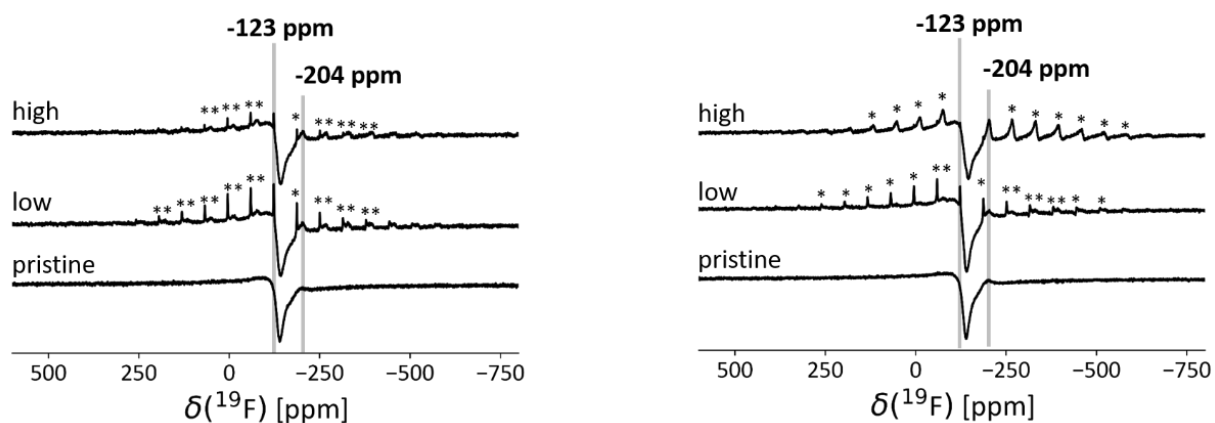


**Figure S13:**  $^{19}\text{F}$  MAS NMR; left) (non-)fluorinated NCM 811 and right) (non-)fluorinated NCM 851005 of pristine, low and high fluorinated NCM CAMs. Spinning sidebands are marked by \*.

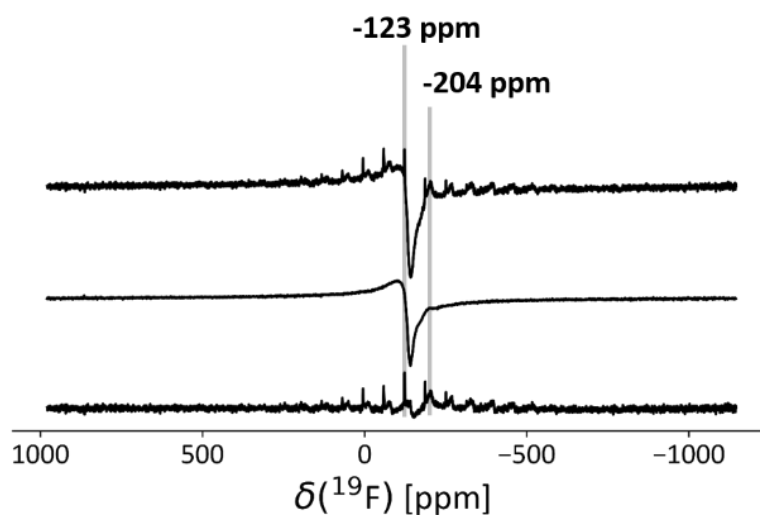


**Figure S14:**  $^{19}\text{F}$  Hahn Echo MAS-NMR spectrum of high fluorinated NCM 811 (30 kHz spinning, r.t., 2.5 mm rotor, 470.65 MHz). The top spectrum shows the signal as recorded, the middle spectrum the background signal arising from PTFE parts of the probe and the bottom spectrum is the difference of the two.

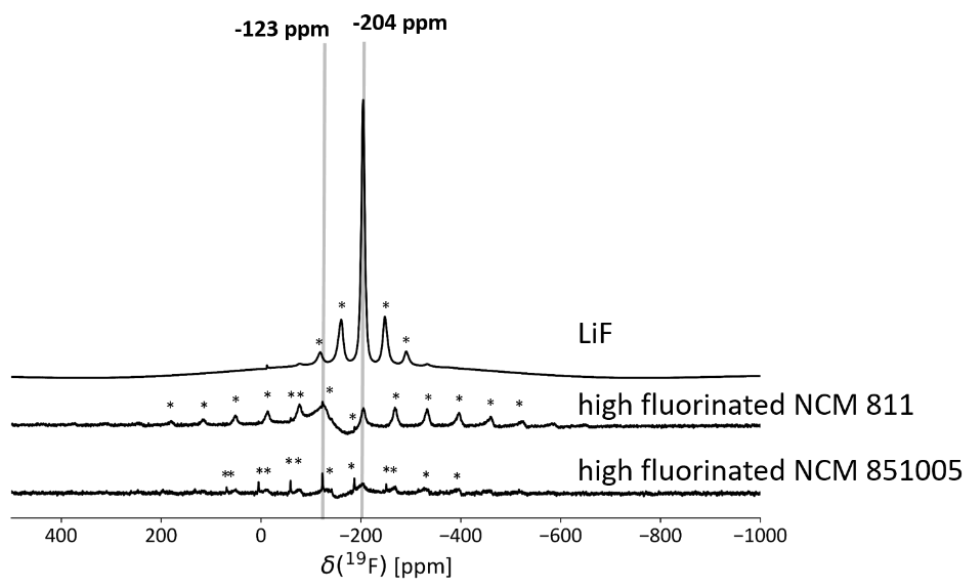


**Figure S15:**  $^{19}\text{F}$  Hahn Echo MAS-NMR spectra of LiF (20 kHz spinning) and high fluorinated Ni-rich NCM materials (30 kHz spinning, background subtracted). Spinning sidebands are marked by \*.

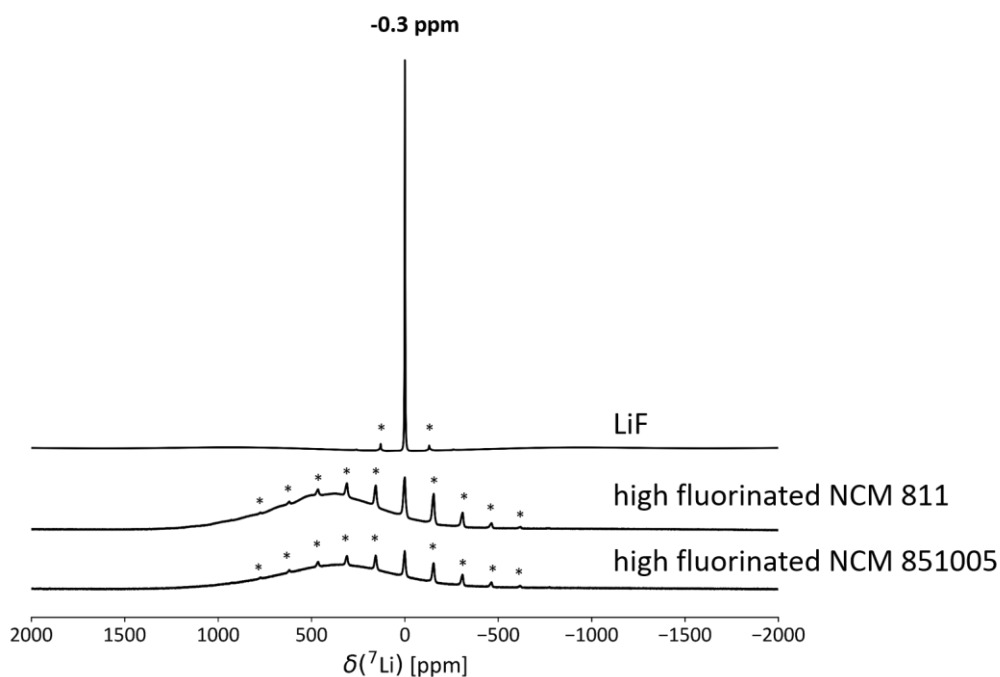


**Figure S16:**  $^7\text{Li}$  solid-echo MAS NMR spectra of LiF (20 kHz spinning) and high fluorinated Ni-rich NCM Material (30 kHz spinning). Spinning sidebands are marked by \*.

### Conductivity measurements of the Ni-rich materials

These measurements were carried out for the pristine and the little fluorinated NCM 811 and NCM 851005 CAMs (Figure S17 and Table S6). For the NCM 811 material: all three samples (pristine, 0.11 wt-% F, and 0.13 wt-% F) show a linear increasing of the conductivity from 2 MPa to 20 MPa. Both fluorinated samples show almost identical results (conductivity vs. pressure), yet the pristine material showed the highest overall conductivities result. The (non-)fluorinated NCM 851005 CAMs

shown almost the same conductivity at 2 MPa with a linear increase of the conductivity vs. pressure until at 20 MPa for all samples. The pristine material showed the best result, followed by the 1.17 wt-% fluorinated material. The results of the four fluorinated samples (0.05 wt-%, 0.58 wt-%, 0.86 wt-%, and 1.44 wt-%) are almost identical.

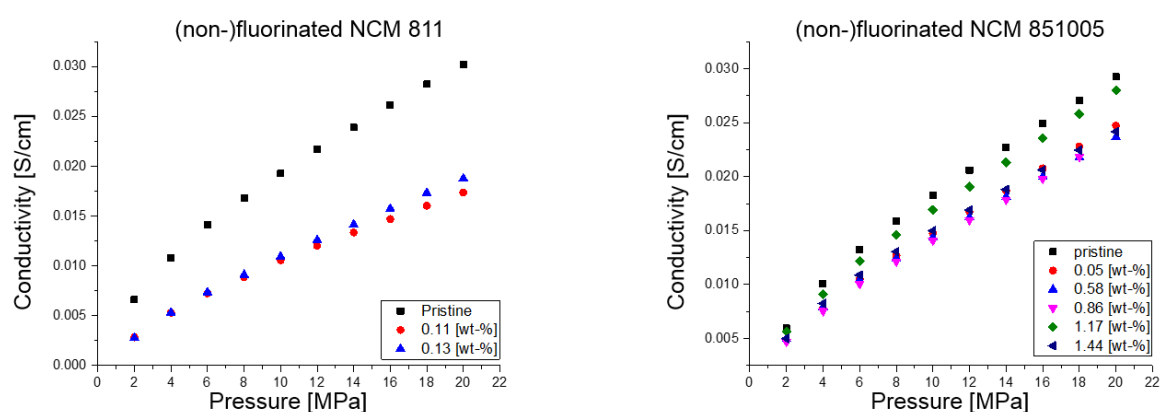


**Figure S17:** Conductivity measurements of (non-)fluorinated Ni-rich materials, left) NCM 811 and right) NCM 851005.

**Table S6:** Conductivity measurements of (non-)fluorinated Ni-rich materials.

Pressure [MPa]	(non-)fluorinated NCM 811			(non-)fluorinated NCM 851005					
	Pristine [S/cm]	0.11 wt-% F [S/cm]	0.13 wt-% F [S/cm]	Pristine [S/cm]	0.05 wt-% F [S/cm]	0.58 wt-% F [S/cm]	0.86 wt-% F [S/cm]	1.17 wt-% F [S/cm]	1.44 wt-% F [S/cm]
2	0.00663	0.00285	0.00278	0.00595	0.00483	0.00495	0.00469	0.00565	0.005
4	0.01079	0.00529	0.00531	0.01008	0.00779	0.00789	0.00755	0.00911	0.00825
6	0.01409	0.00723	0.00736	0.01323	0.01052	0.01043	0.01005	0.01219	0.01089
8	0.01681	0.00885	0.00911	0.0159	0.01268	0.01241	0.01213	0.01462	0.01306
10	0.01927	0.01056	0.01095	0.01829	0.01475	0.01436	0.01407	0.01692	0.01499
12	0.02168	0.01201	0.01259	0.0206	0.01674	0.0162	0.01597	0.01905	0.01692
14	0.02388	0.01334	0.01416	0.02271	0.0187	0.01812	0.01786	0.02133	0.01882
16	0.02614	0.01469	0.01575	0.02491	0.02076	0.01996	0.0198	0.02356	0.02062
18	0.02822	0.01603	0.01733	0.02706	0.02279	0.02179	0.02184	0.02581	0.02245
20	0.03021	0.01736	0.01877	0.02924	0.02472	0.02365	no data	0.028	0.02417

### Press density measurements of the Ni-rich NCM CAMs

These measurements were carried out for several (non-)fluorinated NCM 811 and NCM 851005 samples (Figure S18 and Table S7). All samples show a linear increase of the density with increasing pressure. Yet, all fluorinated samples show consistently higher Press densities at all pressures than the pristine material. The fluorinated NCM 851005 sample with the fluorine concentration of 1.17 wt-% showed the highest Press density values, followed by the 1.44 wt-% fluorinated sample. The best Press densities are by up to 34 % higher than those of the pristine material (Table S7). The

lower fluorinated samples (0.05...0.86 %) showed considerably lower, but still better densities than the pristine material.

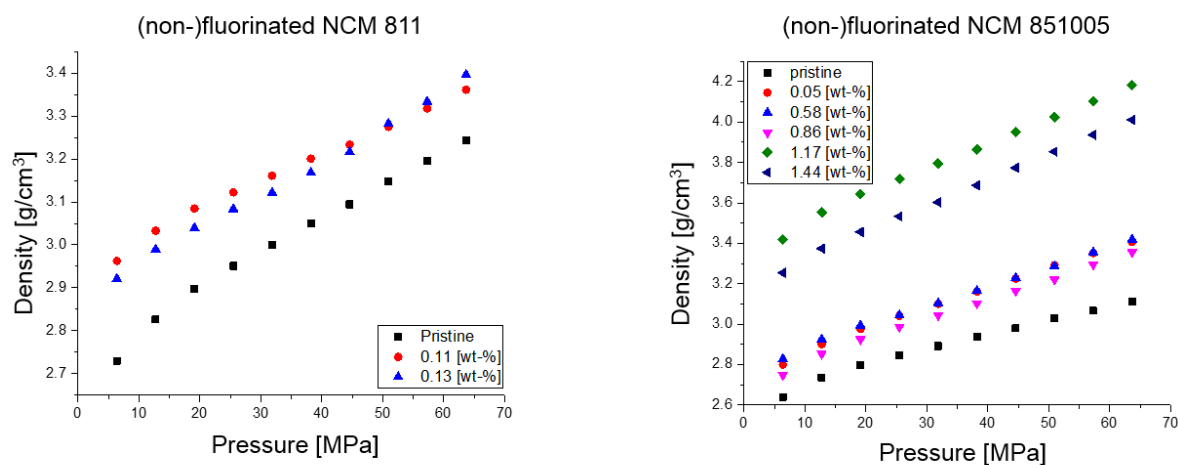


Figure S18: Press density measurements of (non-)fluorinated NCM 811 (left) and NCM 851005 (right).

Table S7: Press density measurements of (non-)fluorinated NCM 811 and NCM 851005.

Pressure [MPa]	(non-)fluorinated NCM 811			(non-)fluorinated NCM 851005					
	Pristine [g/cm <sup>3</sup> ]	0.11 wt-% F [g/cm <sup>3</sup> ]	0.13 wt-% F [g/cm <sup>3</sup> ]	Pristine [g/cm <sup>3</sup> ]	0.05 wt-% F [g/cm <sup>3</sup> ]	0.58 wt-% F [g/cm <sup>3</sup> ]	0.86 wt-% F [g/cm <sup>3</sup> ]	1.17 wt-% F [g/cm <sup>3</sup> ]	1.44 wt-% F [g/cm <sup>3</sup> ]
6.3662	2.72983	2.9625	2.921	2.63959	2.79973	2.82809	2.74817	3.41841	3.25374
12.7324	2.82668	3.03304	2.98957	2.7361	2.90177	2.92538	2.85268	3.55209	3.37425
19.09859	2.89734	3.08445	3.03952	2.79623	2.97635	2.99406	2.92465	3.64369	3.45655
25.46479	2.951	3.12225	3.08368	2.84627	3.04028	3.04408	2.9863	3.71827	3.53315
31.83099	2.9996	3.16098	3.12147	2.89156	3.09946	3.10333	3.04332	3.79596	3.60302
38.19719	3.04984	3.20069	3.16805	2.9383	3.16098	3.16493	3.10255	3.86519	3.68632
44.56338	3.09425	3.23319	3.21606	2.97959	3.225	3.22903	3.16414	3.94922	3.77357
50.92958	3.14773	3.27475	3.28237	3.02925	3.29167	3.28729	3.22007	4.0242	3.85338
57.29578	3.19507	3.31739	3.33392	3.06575	3.35231	3.35649	3.29496	4.10209	3.93663
63.66198	3.24385	3.36115	3.39615	3.11072	3.40609	3.41948	3.35566	4.18305	4.0109

### Thermodynamics of Fluoride Uptake

Reaction equations 1 to 16 in the main text showed the evaluated thermodynamic data for the analysis of the enthalpies of reaction of elementary fluorine gas with the NCBH and SBC layer as well as their side reactions. Below we include the enthalpies of formation  $\Delta_f H^0$  are given in kJ mol<sup>-1</sup>. This data shows that fluorine gas can react thermodynamically with the NCBH and SBC layer, which both are localized on the surface of the material.

Enthalpies of Formation  $\Delta_f H^\circ$  and  $\Delta_f S^\circ$  from Ref. [8] or the National Institute of Standards and Technology Website at <https://webbook.nist.gov/chemistry/name-ser/>

Compound	$\Delta_f H^\circ$ [kJ/mol]	$\Delta_f S^\circ$ [J/K mol]	Compound	$\Delta_f H^\circ$ [kJ/mol]	$\Delta_f S^\circ$ [J/K mol]
NiO(s)	-240.0	43.7	LiOH(s)	-441.5	
CoO(s)	-237.9	53.0	Li <sub>2</sub> O(s)	-561.2	
MnO(s)	-385.2	59.7	Li <sub>2</sub> CO <sub>3</sub> (s)	-1132.	
Mn <sub>2</sub> O <sub>3</sub> (s)	-959.0	110.5	LiF(s)	-587.7	
MnO <sub>2</sub> (s)	-520.0	53.1	F <sub>2</sub> (g)	0.0	202.8
Ni <sub>2</sub> O <sub>3</sub> (s)	-489.5		O <sub>2</sub> (g)	0.0	205.2
Ni(OH) <sub>2</sub> (s)	-538.0	79.0	HF(g)	-275.4	173.8
Co(OH) <sub>2</sub> (s)	-539.7	79.0	H <sub>2</sub> O(l)	-285.8	70.0
Co <sub>3</sub> O <sub>4</sub> (s)	-891.0	102.5	H <sub>2</sub> O(g)	-241.8	188.8
CoCO <sub>3</sub> (s)	-713.0	91.7	CO <sub>2</sub> (g)	-394.4	213.8
MnCO <sub>3</sub> (s)	-894.1	85.8	MnF <sub>2</sub> (s)	-855.0 <sup>a)</sup>	
NiF <sub>2</sub> (s)	-651.4	73.6			
CoF <sub>2</sub> (s)	-671.5	82.0			
CoF <sub>3</sub> (s)	-790.4	94.5			

<sup>a)</sup> From Jacob, K. T.; Hajra, J. P. (1987): Measurement of Gibbs energies of formation of CoF<sub>2</sub> and MnF<sub>2</sub> using a new composite dispersed solid electrolyte. In: Bull. Mater. Sci. 9 (1), S. 37–46. DOI: 10.1007/BF02744391.

## References

- [1] A.C. Larson and R.B. Von Dreele, *General Structure Analysis System (GSAS)*. Los Alamos National Laboratory Report LAUR 86-748, **2004**.
- [2] B. H. Toby, *J Appl Crystallogr* **2001**, 34, 210.
- [3] E. G. Reilly, *Review of Scientific Instruments* **1953**, 24, 875.
- [4] Acros Organics, "Material Safety Data Sheet of MnF<sub>3</sub>".
- [5] Alfa Aesar, "Sicherheitsdatenblatt (Material Safety Data Sheet) of LiF", **2013**.
- [6] Alfa Aesar, "Sicherheitsdatenblatt (Material Safety Data Sheet) of NiF<sub>2</sub>", **2014**.
- [7] Carl Roth, "Sicherheitsdatenblatt (Material Safety Data Sheet) of LiF", **2015**.
- [8] D. R. Lide (Ed.) *CRC handbook of chemistry and physics. A ready-reference book of chemical and physical data*, CRC Press, Boca Raton, Fla., **1997**.
- [9] Merck Group, "Sicherheitsdatenblatt (Material Safety Data Sheet) of LiF", **2015**.
- [10] SCS GmbH, "Sicherheitsdatenblatt (Material Safety Data Sheet) of LiF", **2012**.
- [11] SIGMA-ALDRICH, "Sicherheitsdatenblatt (Material Safety Data Sheet) of LiF", **2016**.
- [12] SIGMA-ALDRICH, "Sicherheitsdatenblatt (Material Safety Data Sheet) of NiF<sub>2</sub>", **2016**.
- [13] Thermo Fisher Scientific, "Sicherheitsdatenblätter (Material Safety Data Sheet) of MnF<sub>3</sub>", **2017**.
- [14] K. Nakamoto, *Infrared and Raman spectra of inorganic and coordination compounds. Part A: Theory and applications in inorganic chemistry*, Wiley, Hoboken, N.J., **2009**.
- [15] U. Breddemann, E. M. Erickson, V. Davis, F. Schipper, M. Ellwanger, M. Daub, A. Hoffmann, C. Erk, B. Markovsky, D. Aurbach et al., *ChemElectroChem* **2019**.

- [16] M. Murakami, H. Yamashige, H. Arai, Y. Uchimoto, Z. Ogumi, *Electrochem. Solid-State Lett.* **2011**, *14*, A134.
- [17] M. Ménétrier, J. Bains, L. Croguennec, A. Flambard, E. Bekaert, C. Jordy, P. Biensan, C. Delmas, *J. Solid State Chem.* **2008**, *181*, 3303.
- [18] N. Dupré, J.-F. Martin, D. Guyomard, A. Yamada, R. Kanno, *J. Power Sources* **2009**, *189*, 557.